Journal of South American Earth Sciences xxx (xxxx) 103231

Contents lists available at ScienceDirect

Journal of South American Earth Sciences

journal homepage: www.elsevier.com/locate/jsames

Environmental changes during MIS6-3 in the Basin of Mexico: A record of fire, lake productivity history and vegetation

L.R. Martínez-Abarca [a], S. Lozano-García [a, *], B. Ortega-Guerrero [b], C.M. Chávez-Lara [a], E. Torres-Rodríguez [a], M. Caballero [c], E.T. Brown [c], S. Sosa-Nájera [a], C. Acosta-Noriega [d], V. Sandoval-Ibarra [a]

[a] Instituto de Geología, Universidad Nacional Autónoma de Mexico, Ciudad Universitaria, CP 04510, Ciudad de Mexico, Mexico
[b] Instituto de Geofísica, Universidad Nacional Autónoma de Mexico, Ciudad Universitaria, CP 04510, Ciudad de Mexico, Mexico
[c] Large Lakes Observatory & Dept. of Earth and Environmental Sciences, University of Minnesota Duluth, Duluth, MN, 55812, USA
[d] Posgrado en Ciencias Biológicas, Universidad Nacional Autónoma de Mexico, Ciudad Universitaria, CP 04510, Ciudad de Mexico, Mexico

ARTICLE INFO

Keywords:
Lake Chalco
Glacial-interglacial
North America
Fire-activity
Palynology
Z-Score analysis

ABSTRACT

The responses of lake productivity, vegetation, and fire events in the Basin of Mexico to orbital changes from late MIS 6 to MIS 3 (146–35 ka) have been studied based on geochemical (Ti, TIC, TOC, C/N), charcoal (CHAR) and pollen data of the sediment core CHA08 from Lake Chalco. The paleoenvironmental reconstruction identifies the MIS 6 as a wetter period with episodes of dry conditions, low forest cover and low fire activity. A sudden change from wetter to dry environments with low to high forest cover and fire activity episodes characterized the end of the MIS 6 (132–130 ka) coincident with high spring insolation. Variations in vegetation composition, with a tendency towards higher forest cover, fire-activity, runoff, and organic matter availability, are recorded during the MIS 5, MIS 4, and MIS 3. However, a reduction in the fire-activity was recorded for the cold and dry MIS 4. Spectral analysis based on the titanium concentration record of Lake Chalco suggests a precessional forcing on runoff variations. We explored the impact of the Intertropical Convergence Zone latitudinal migrations which have been related to the summer insolation at 65 N by comparing runoff data with other sedimentary records from North and Central America. Our results highlight the sensitivity of the high altitude tropical basin to climate variations.

1. Introduction

Major climate fluctuations of the Late Quaternary led to shifts in the isotopic composition of global seawater that were recorded in marine carbonates and have been utilized to define Marine Isotope Stages (MIS) (Emiliani, 1955; Schackleton, 1967; Dansgaard et al., 1993; Lisiecki and Raymo, 2005). On the continents, these are manifested as alternations between glacial (e.g. MIS6 and MIS2) and interglacial conditions (e.g. MIS5 and MIS1) and have been recognized globally (Watts et al., 2000; Guiter et al., 2003; Heusser and Oppo, 2003; Muhs et al., 2003; Yang et al., 2006; Cai et al., 2010; Moreno et al., 2012).

Records from Central America and southwestern North America suggest that MIS6 conditions were dry and cold, with large herbaceous communities and low recurrence of fires (Hanselman et al. 2005, 2011; Bogotá et al., 2011; Macario-Gonzalez, 2017). Contrary to this, the MIS5 climate is considered warmer, and five sub-stages have been proposed with variable temperature and moisture conditions (Lisiecki and Raymo, 2005). During MIS5e, global temperature and sea levels increased >4 °C and 120 m, respectively (Guiter et al., 2003; Muhs et al., 2003). In Central America and southwestern North America woodland communities' composition changed drastically, with open pine forests as the main vegetation type (Cárdenes-Sandí et al., 2019; Anderson et al., 2020). Sub-stages MIS5d and 5b were slightly drier and colder than MIS5c and 5a. It has been proposed that the MIS4 climate was cold in several parts of this region (Bogotá et al., 2011; Glover et al., 2017; Macario-Gonzalez, 2017). The beginning of MIS4 was drier than the end, and a higher recurrence of fires is registered in temperate regions from North America (Anderson et al., 2020; Glover et al., 2020). The MIS3 was warmer and wetter than MIS4, favoring the development of large fluvial systems and extended boreal communities with higher fire recurrence in Central America and southwestern North America (Bush et al., 2009; Vriend et al., 2012; Glover et al., 2017).

* Corresponding author.
E-mail address: mslozano@unam.mx (S. Lozano-García).

https://doi.org/10.1016/j.jsames.2021.103231
Received 21 December 2020; Accepted 14 February 2021
0895-9811/

Lake Chalco (Central Mexico), located between the tropical equatorial zone and the North Hemisphere temperate region, represents a key site for paleoclimate research due to its location between the tropical equatorial zone and the North Hemisphere temperate region. This lake preserves the paleoclimatic history over the last 400 kyr in the sedimentary record, representing one of the longest archives from the Neotropics (Lozano-García et al., 2017; Brown et al., 2019; Martínez-Abarca, 2019a). Since the 1990s, Lake Chalco has been the subject of several studies characterizing the climatic and limnological variability during the last 150 kyr, with a focus on the past 40 kyr (e.g. Lozano and Ortega, 1998; Lozano-García et al., 2015; Ortega-Guerrero et al., 2017; Caballero et al., 2019; Ortega-Guerrero et al., 2020). Previous studies have revealed that Lake Chalco exhibited significant variations in lacustrine levels, redox conditions, and salinity since MIS6 (Avendaño-Villeda et al., 2018; Torres-Rodríguez et al., 2018; Ortega-Guerrero et al., 2020). Moreover, significant moisture and temperature changes have been recognized, with the MIS2 the coldest period of this region (Caballero et al., 2019). Additionally, changes in the plant cover and composition and evidence of paleo fire-activity in the sedimentary records of Lake Chalco have been documented principally for the last 40 kyr (Lozano-García et al., 1993; Lozano-García 1996; Torres-Rodríguez et al., 2015; Martínez-Abarca et al., 2019b).

Building on previous work carried out at Lake Chalco, in this work, we explore environmental responses of the Basin of Mexico examining records of fire, forest cover, and lake productivity between the end of MIS6 and the beginning of MIS3 (143–35 ka). We discuss whether variation in the fire production and organic matter input results from global or regional factors, such as changes in runoff, evaporation, vegetation cover and insolation at the Basin of Mexico. Furthermore, we compare our results with other records such as Lake Baldwin (USA), Cariaco Basin (Venezuela) and the marine core ODP 1239 (Ecuador) to generate an overview of regional climatic variability.

2. Regional setting

Lake Chalco is located at the Transmexican Volcanic Belt (TMVB) southeastern area in the south portion of Basin of Mexico (Fig. 1), where in prehispanic times a large ancient lake system was established. The lake have had important transformations and currently the modern remnant lake is a shallow marsh (< 3 m depth; < 6 km^2) at the southern edge of the Mexico City metropolitan area (19 150 N, 98 58' W, 2230 m asl) (Ortega-Guerrero et al., 2020). Lake Chalco is a depocenter fed by the Sierra Nevada Mountains in the east, the Sierra de Santa Catarina Mountains in the north and the Sierra Chichinautzin Mountains in the south. Pleistocene and Holocene andesite and dacite from Chichinautzin and the Sierra Nevada are the dominant lithology around the lake. The second dominant lithology consists of Quaternary deposits such as lacustrine sediments and alluvium.

The climate is high altitude subtropical temperate (Cw). The rainy season occurs during the summer and a dry season from December to April. During the rainy season, the Intertropical Convergence Zone (ITCZ) is located at its northernmost position providing rain to Mexico's central and southern regions. As the ITCZ moves southwards, most of Mexican territory experiences drought. (*Comisión Nacional Forestal* [CONAFOR], 2020), although polar fronts can deliver precipitation during the dry season (Lozano-García et al., 1993).

Most fires in Mexico mainly occur at the end of winter and during the first weeks of spring. At present, these are nearly entirely anthropogenic with only 2% of fires initiated by natural causes (CONAFOR, 2020). Previous studies in Chalco suggest a variable fire-activity and climatic conditions associated to ITCZ position variation during the last 40 kyr (e.g. Lozano-García et al., 2015; Torres-Rodríguez et al., 2015; Martínez-Abarca et al., 2019b; Caballero et al., 2019).

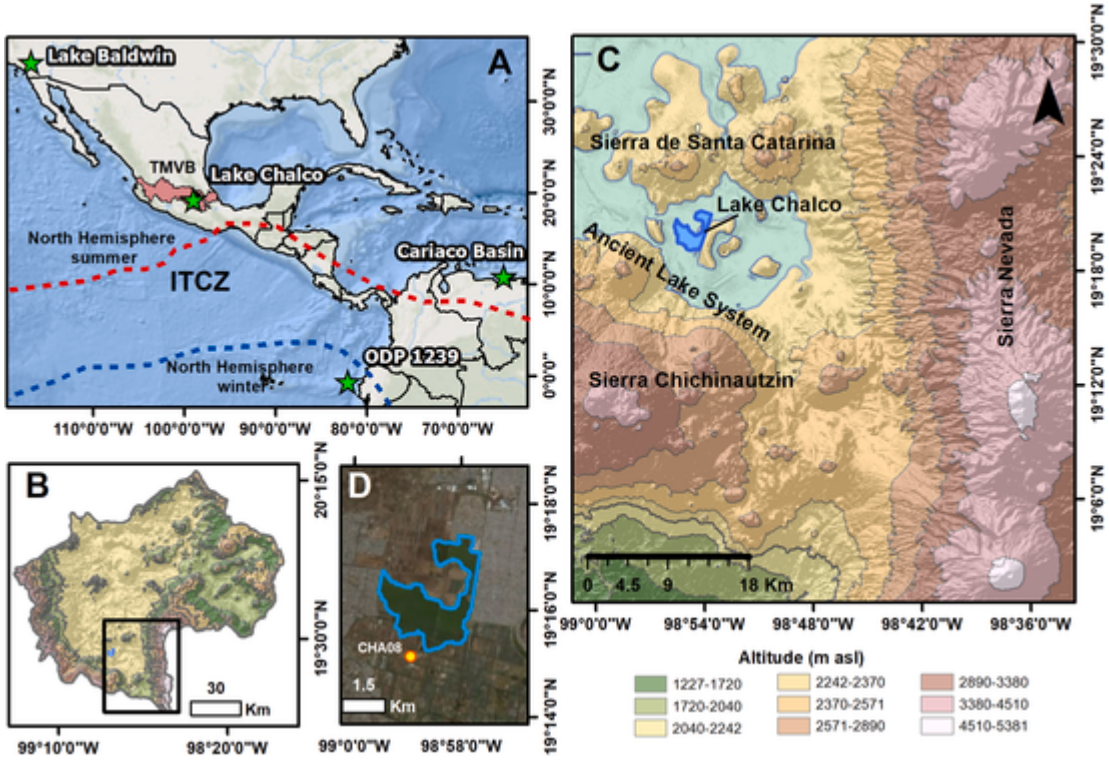

Fig. 1. Map of Lake Chalco location: A) Transmexican Volcanic Belt (TMVB), Basin of Mexico and Intertropical Convergence Zone (ITCZ) mean position during summer and winter months for the North Hemisphere. We also show some North Hemisphere records that will be discussed; B) Basin of Mexico and southern Lake Chalco location; C) Chalco sub-basin elevation model and location of Sierra de Santa Catarina, Sierra Nevada and Sierra Chichinautzin mountains (INEGI, 2020); D) Lake Chalco satellite image, the drill site CHA08 is indicated with a yellow dot (Google Earth Pro, 2020). (For interpretation of the references to color in this figure legend, the reader is referred to the Web version of this article.)

3. Material and methodology

3.1. Drilling and stratigraphy

In 2008, three overlapping cores drilled from the depocenter zone of the ancient Lake Chalco: CHA08-IV (85–122 m), CHA08-V (29–72 m) and CHA08-VI (70.8–85 m and 106–122.4 m) yielded sedimentary records representing the sequence between 29 and 122.4 m depth. Sediments were recovered with a Shelby corer in 1.10 m long sections with inner PVC tubes 1 m long and 10 cm in diameter; the remaining 10 cm were collected from the drilling shoe. Initial measurements and core descriptions were carried out at the LacCore facility (University of Minnesota Twin Cities). A composite depth model for the three cores was developed on the basis of stratigraphic features, tephra markers, and magnetic susceptibility profiles. Seven lithostratigraphic units along 122.4 m were identified by Ortega-Guerrero et al. (2017). In this work, we only focus on Units 4–7 (29–122.4 m depth). More details about lithostratigraphy and facies characteristics can be found in Ortega-Guerrero et al. (2017; 2020).

3.2. Chronology

The age-depth model (Fig. 2) here presented has been previously described by Ortega-Guerrero et al. (2017). Overall, a Bayesian model was carried out through free distribution R-Studio software and Bacon package (Blaauw and Christen, 2011; R Core Team, 2018). Fourteen radiocarbon ages calibrated by the IntCal13 curve (Reimer et al., 2013) were considered for the upper 35 m, as well as age of two tephra deposits: Upper Toluca Pumice and Tutti Frutti Pumice (Arce et al., 2003; García-Palomo et al., 2012; Sosa-Ceballos et al., 2012) recognized in the Basin of Mexico. Additional age constraints, beyond the radiocarbon range include a $^{230}Th/U$ age from zircon extracted at 63.5 m depth (Torres-Rodríguez et al., 2015) and an age of 130 ka at 106 m based on stratigraphic and diatom analyses (Avendaño-Villeda et al., 2018) hypothesized to represent the transition between MIS6 and MIS5 (Lisiecky and Raymo, 2005) (Table 1).

3.3. Charcoal analysis

Charcoal analyses were carried out in sediments from semi-regular intervals (between 20 and 25 cm) along the stratigraphic sequence. Samples of 0.5 cm^3 were dissolved in a 10% $Na_4P_2O_7$ solution and heated to 40 °C for organic matter disaggregation. Clay was removed by 53 μm mesh sieving and the remaining charcoal particles were photographed under a stereoscopic microscope with ×1.6 magnification. Images were processed by ImageJ free software, quantifying total particle area. Charcoal concentration [mm^2/cm^3] and charcoal accumulation rate (CHAR) [mm^2/cm^2yr] were calculated based on the quantified area. Low and high-frequency components of the CHAR were isolated through Z-Score analyses processed by R Studio free software (R Core Team, 2018). Additionally, the percentages of particles >100 μm (primary signal) and <100 μm (secondary signal) were calculated for samples between 85 and 122 m depth.

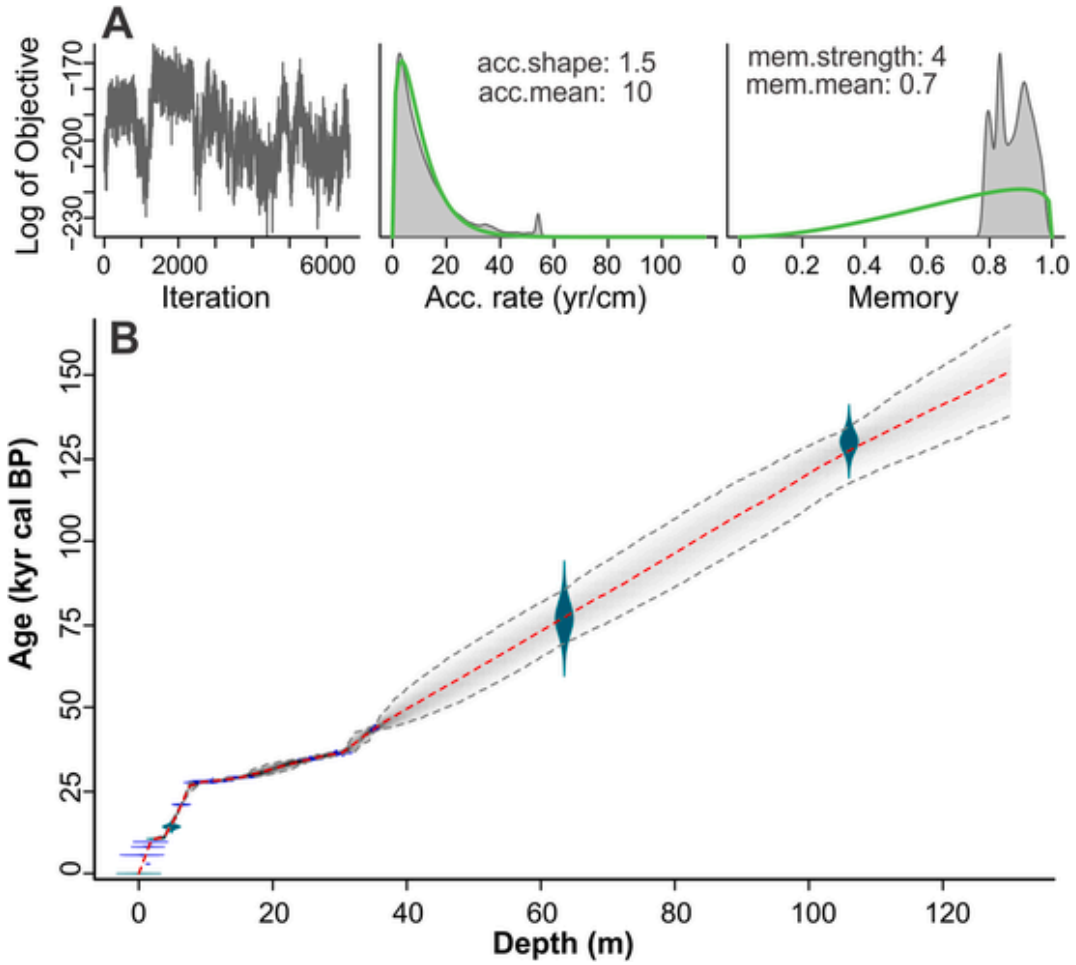

Fig. 2. Bayesian age-depth model obtained for the CHA08 record (Modified from Ortega-Guerrero et al., 2017; 2020): A) Model parameters estimated by energy, accumulation range and memory (from left to right); B) Chronology of CHA08 core.

Table 1
Data used for the Bayesian age-depth model. Asterisk (*) represents ages not obtained by ^{14}C.

Code/Parameter	Depth (m)	Uncalibrated age (BP ± 1σ)	Material dated	Reference
Beta-347500	0.47	4830 ± 30	Pollen	Ortega-Guerrero et al. (2017)
Beta-347502	1.36	7220 ± 30	Ostracods	Ortega-Guerrero et al. (2017)
Beta-347503	1.37	2780 ± 40	Pollen	Ortega-Guerrero et al. (2017)
Beta-347501	1.76	8490 ± 40	Pollen	Ortega-Guerrero et al. (2017)
UTP date	2.53	10445 ± 90	n.a.	Arce et al. (2003) García-Palomo et al. (2002)
PTF date	4.88	14065 ± 500	n.a.	Sosa-Ceballos et al. (2012)
Beta-359187	6.35	17180 ± 60	Pollen	Ortega-Guerrero et al. (2017)
Beta-359191	9.25	23180 ± 90	Pollen	Ortega-Guerrero et al. (2017)
Beta-359189	10.25	23450 ± 100	Pollen	Ortega-Guerrero et al. (2017)
Beta-359190	11.03	23720 ± 110	Pollen	Ortega-Guerrero et al. (2017)
Beta-344189	15.41	24760 ± 100	Pollen	Ortega-Guerrero et al. (2017)
Beta-344190	25.63	29970 ± 180	Pollen	Ortega-Guerrero et al. (2017)
Beta-344191	29.47	31840 ± 230	Pollen	Ortega-Guerrero et al. (2017)
Beta-344192	30.46	31940 ± 210	Pollen	Ortega-Guerrero et al. (2017)
Beta-347499	35.18	40460 ± 520	Ostracods	Ortega-Guerrero et al. (2017)
Th/U*	63.50	76700 ± 4700	Zircons	Torres-Rodríguez et al. (2015)
MIS5-6*	106	130000 ± 3000	n.a.	Avendaño-Villeda et al. (2018) Lisiecki and Raymo (2005)

3.4. Geochemical analyses

Major elemental composition analyses (including Ti) were performed at the Large Lakes Observatory, University of Minnesota Duluth, with a COX ITRAX X-Ray Fluorescence (XRF) core scanner at 1-cm resolution using an X-Ray Mo-tube source configured at 30 kV and 20 mA (more details in Ortega-Guerrero et al., 2020). Measurements obtained as count per second [cps] were calibrated against NIST Standard Reference Materials and the cps data were converted to percentage (%). Additionally, a spectrum analysis through Lomb periodogram algorithm (simple periodogram; Press et al., 1992) was carried out on Ti values for recognizing possible oscillation causes in runoff input. Moreover, the noise signal on the database was previously removed using a LOESS smoothing function with a smoothing factor of 0.06. LOESS analysis was carried out in R-Studio and the Lomb periodogram in Past software (Hammer et al., 2001).

Samples for carbon and nitrogen analyses were dried at 40 °C, homogenized and ground with an agate pestle. Concentrations of total carbon (TC), total organic carbon (TOC) and total nitrogen (TN) were measured with a C/N Flash 2000 analyzer at intervals of 10 cm at the Paleoenvironment and Climate Change laboratory, National Autonomous University of Mexico (UNAM). Using TOC and TN values, we estimated C/N molar ratios. Total inorganic carbon (TIC) was obtained as TIC = TC-TOC. For the discussion section, Ti and TIC percentages were standardized dividing the mean value by the standard deviation of the measured value (e.g. Roy et al., 2013; Kirby et al., 2010).

3.5. Pollen analysis

A total of 355 samples of 0.5 cm^3 sediment were processed for pollen extraction, according to Batten (1999), and one or two *Lycopodium clavatum* spore tablets were added for pollen concentration calculations. 200 grains were quantified, excluding *Pinus* and non-pollen palynomorphs. Identification was performed using the Basin of Mexico Pollen Reference Collection from the Paleoecology, Paleoenvironment, and Climate Change lab at UNAM.

4. Results

Here we show the proxy data analyzed between 29 and 122.4 m depth from CHA08 core (Fig. 3). All data is presented according to the lithostratigraphic units proposed by Ortega-Guerrero et al. (2017). Unit 7 covers from 122.4 to 106 m depth, Unit 6 from 106 to 57.5 m depth, Unit 5 from 57.5 to 41.1 m depth, and Unit 4 from 41.1 to 29 m depth.

Ti concentration ranges from 0.5 to 2.6% with an average of 1.8%. Unit 7, at the bottom of the record, shows the highest amplitude variation of Ti (0.6–2.4%). Unit 6 has relatively high Ti levels (1.2–2.6%), whereas the subsequent unit (Unit 5) presents relatively low concentrations (1.1–2.4%). Unit 4 shows the lowest amplitude variation of Ti concentration with the closest values to average content ranging from 1.0 to 2.4%.

TIC content ranges from 0.0 to 6.6% with an average of 0.9%. Sediments in Unit 7 present overall lower than the average TIC concentrations (0.0–5.4%). Unit 6 and 5 show a relatively similar high amplitude variation pattern ranging from 0.0 to 6.3% and 0.0–6.6%, respectively. Sediments in Unit 4 present the lowest amplitude variation of TIC content (0.0–4.3%).

TOC content ranges from 0.2 to 11.4% with an average of 3.7%. Sediments in Unit 7 present in general lower than the average TOC concentration (0.2–10.3%). Unit 6 shows the highest amplitude variation of TOC concentration (0.3–11.4%), whereas concentration amplitude variation decreases in overlying sediments from Unit 5 and Unit 4, ranging from 0.9 to 6.5% and 0.2–6.9%, respectively.

TN concentration varies from 0.0 to 0.7% and sediments exhibit C/N (TOC/TN) ratio values varying from 3.6 to 38.8. In Unit 7 C/N is low, typically ≤10, whereas sediments in the other units (Unit 6, 5 and 4) exhibit C/N ≥ 10 values with the highest peak in Unit 5 at 51.6 m depth.

Charcoal concentrations range from 0.0 to 71.5 mm^2/cm^3 with the lowest values in the deepest part of the sequence, and the highest value at 59.3 m. Fig. 4 shows the CHAR dataset and peaks detected by Z-Score analysis. CHAR oscillates from 0.0 to 83.8 mm^2/cm^2yr and, as concentration data, increases to the upper section. In Unit 7 we detected lower Z-Score values (up to 1.3) and scarce peaks (6 detected), whereas in the upper units they increased up to 6.9, 6.1 and 4.3 in Unit 6, 5 and 4, respectively. Unit 6 presents the highest peak number detected by Z-Score analysis (111 peaks).

Pollen data is presented as percentages in Fig. 4, showing only the relationship between the arboreal pollen and non-arboreal. At Unit 7 the non-arboreal pollen attains the highest values (25–52%). The non-arboreal pollen percentage decreases in Unit 6, and in Unit 5 and 4 exhibits the lowest values of the record.

5. Discussion

5.1. Proxy interpretation

TOC content in bulk sediment reflects the amount of primary productivity (Cohen, 2003), whereas the C/N mass ratio reflects the contribution of terrestrial vegetation and lacustrine algae on the deposited organic matter (Meyers and Ishiwatari, 1995). Lacustrine algae and

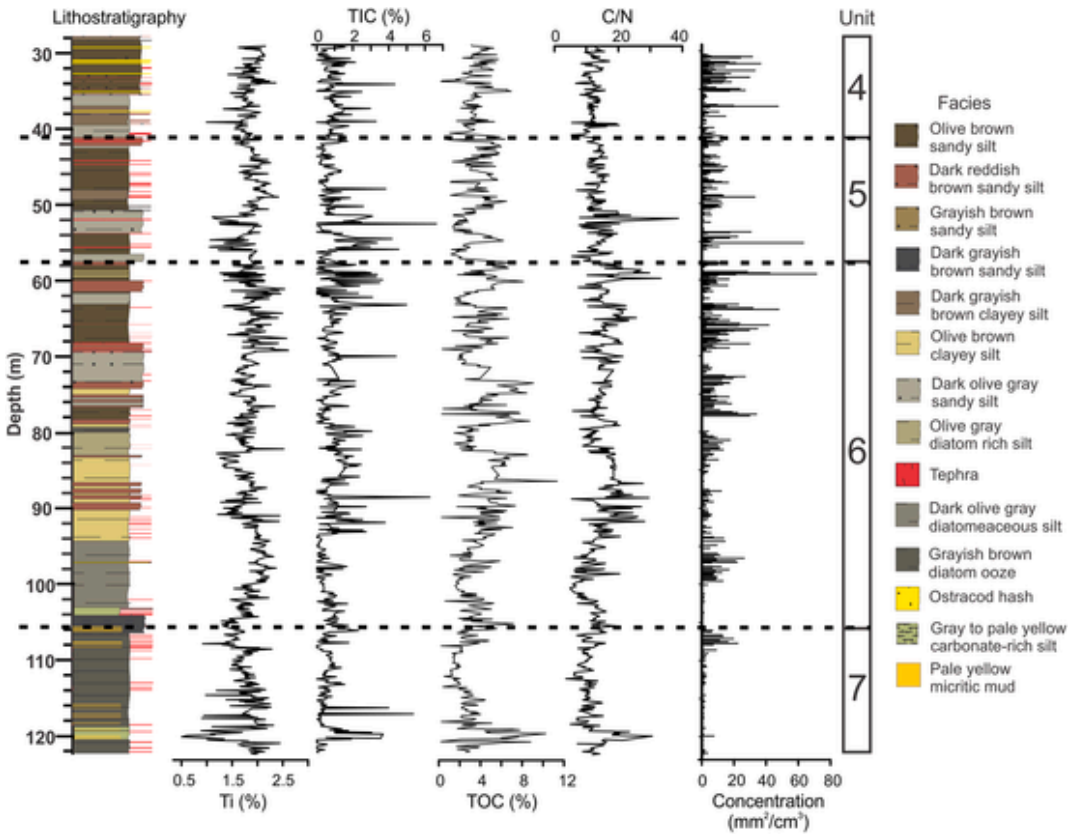

Fig. 3. Lithostratigraphy and proxy data of the sedimentary record CHA08 between 122.4 and 29 m depth. These include Ti percentages, total inorganic carbon percentages (TIC), total organic carbon content (TOC), C/N ratio and Charcoal concentrations. Results are presented with the sedimentary units of Ortega-Guerrero et al. (2017).

terrestrial plants have differing nitrogen contents, so organic material with lower C/N (<10) is primarily from aquatic plants, whereas higher C/N (>10) indicates that the organic matter mainly from terrestrial sources (Talbot and Johannessen, 1992; Meyers and Ishiwatari, 1995; Cohen, 2003). Organic matter with contributions from both lacustrine and terrestrial sources has C/N values between 10 and 20. However, for a more specific determination of the organic matter source in sediments, lipid biomarkers analysis would be necessary for determining algal and bacterial biomass, aquatic microfauna and surrounding vegetation organic matter variable input.

Titanium (Ti) is an insoluble element, essentially immobile in chemical weathering, and it does not respond to environmental redox variation. This means that Ti does not reprecipitate as authigenic fraction nor can be adsorbed into clay minerals (Mason and Moore, 1982; Yarincik et al., 2000; Boyle, 2002). Ti also represents the abundance of mafic and heavy minerals in the sediments. The Ti content of sediments may be considered a proxy indicator of runoff as in the Basin of Mexico the main watershed rocks are volcanic with intermediate composition (Delgado Granados and Martin del Pozzo, 1999; Arce et al., 2019).

There are no surface exposures of carbonate-bearing exposed rocks in the Chalco watershed. Therefore, we consider carbonate-enriched sediments (high TIC concentrations) to have been deposited during intervals of higher salinity associated with relatively arid conditions (Torres-Rodríguez et al., 2015).

CHAR data is an indicator of fire-activity (Whitlock and Larsen, 2001), which, in turn, is impacted by multiple factors. Long term records indicate that fire-activity in the Basin of Mexico depends on drought, spring insolation, and abundance of vegetation/fuel (Torres-Rodríguez et al., 2015). We use low Ti levels coupled with high TIC concentrations as indicators of drought periods. In addition, we use the 20°N spring and summer insolation curves to visually relate charcoal maximum with insolation variation. Furthermore, arboreal/non-arboreal pollen percentages are used as an indicator of forest cover and hence for fuel availability (Tinner and Hu, 2003).

To evaluate proximity of fires, CHAR was separated into high and low frequency components through Z-Score analysis, a normal distribution test that estimates the standard deviation from average data. The high frequency (also called peak signal) is associated with local fires occurring in the immediate lake area (Oris et al., 2014). Most of the peak signal is composed of primary charcoal particles (>100 μm diameter). On the other hand, the low frequency background signal, typically composed of secondary charcoal particles (<100 μm diameter) (Whitlock and Millspaugh, 1996), is usually associated with more distant regional fires, as well as charcoal transported by slope-wash processes (water and wind) (Whitlock and Larsen, 2001; Oris et al., 2014). LOESS polynomial regressions may be used to examine charcoal distributions in lakes with relatively constant sedimentation rates that are modified during fire events (e.g. Clark and Royall, 1996; Long et al., 1998; Higuera et al., 2007). It has been previously applied in studies of Chalco sediments (e.g. Torres-Rodríguez et al., 2015; Martínez-Abarca et al., 2019b). However, the charcoal accumulation rate in central Mexico is variable due to the diversity of vegetation, well-marked changes in the microclimate between regions, and volcanic and tectonic processes (López-Pérez, 2014). Therefore, in this paper, we present Z-Score analysis as a new method for separating high and low charcoal frequency in the region as it is independent of charcoal accumulation rates and sampling resolution (Brücher et al., 2014; Glantz et al., 2016). Positive Z-Score values are the peak signal and in consequence can be interpreted as local fires (e.g. Power et al., 2008; Brücher et al., 2014; Leunda et al., 2020).

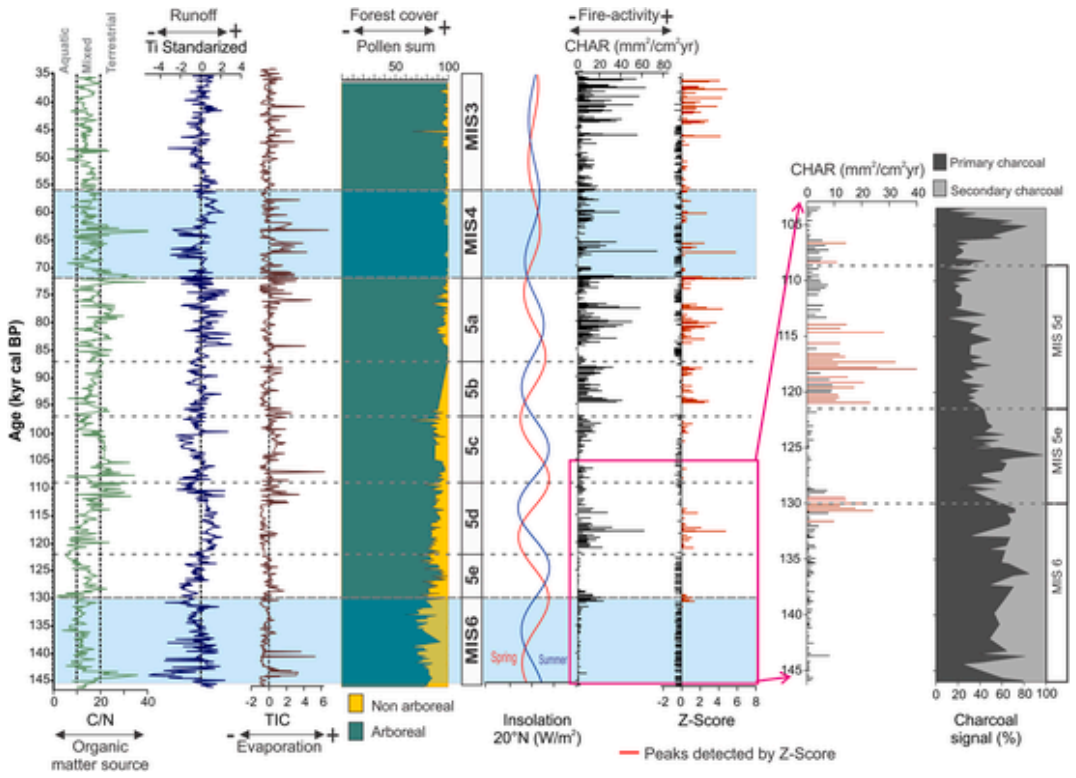

Fig. 4. Comparison of proxy records of CHA08 sequence between 143 and 35 ka divided by grey horizontal dotted lines indicating the transition between different stages and sub-stages. Light blue shades indicate periods of colder conditions. It is showed: 1) Total organic carbon to total nitrogen ratio (C/N) as a marker of organic matter source, 2) standardized Ti as an indicator of runoff, where grey dotted line represents mean value, 3) TIC percentage as a marker of evaporation rate, 4) Pollen data (arboreal/non-arboreal percentages), 5) Spring and summer insolation variation at 20°N, 6) CHAR data that indicates paleo-fire activity, 7) Z-Score results where local fires are marked as red bars and separated from regional fires (black bars). Additionally, a close-up of the CHAR data and peaks detected during MIS6, MIS5e and MIS5d, and the percentage of primary and secondary particles present in the sediment is shown. (For interpretation of the references to color in this figure legend, the reader is referred to the Web version of this article.)

5.2. The environmental history of Lake Chalco during MIS6-MIS3

5.2.1. Marine Isotope Stage 6 (146–130 ka)

The deepest section corresponds with the last part of the Marine Isotope Stage 6 (MIS6) between 146 and 130 ka (122.4–106 m; Unit 7; Fig. 4). Previous studies based on magnetic minerals composition and diatoms content suggest the Chalco Basin was occupied by a deep, freshwater, anoxic, relatively cold and eutrophic lake in an environment colder than MIS2 (Avendaño-Villeda et al., 2018; Ortega-Guerrero et al., 2020; Avendaño-Villeda et al. in revision).

During this period, low C/N and low TIC suggest conditions of a highly productive lake and low evaporation rate confirming previous reconstructions made in Chalco (e.g. Ortega-Guerrero et al., 2020). Increasing values of TIC and a drop in Ti between 145.2 and 143 ka suggest a period of dryer conditions (lower runoff) with relatively higher evaporation rate. These might have caused a drop in lake level around ca. 144 ka, promoting occurrence of emergent plants with higher C/N (e.g. Chávez-Lara et al., 2019). Low CHAR values (0.0–8.2 mm^2/cm^2yr) suggest a low fire-activity despite dry conditions. However, particle signal data shows a high percentage of primary charcoal (50–80%) along MIS6, indicating that fire activity was close to the lake (Fig. 4). The low recurrence of fires during MIS6 can be related to two possible factors. The first could be the establishment of open forest as indicated by the low forest cover with abundant non-arboreal vegetation (representing low fuel availability). Nowadays, most plant communities in the region are represented by forests with several *Pinus* species and *Abies,* and *Quercus* communities where fire plays an important role (Lozano-García, 1996). High values of non-arboreal vegetation suggest the establishment of grasslands in response to colder conditions at the basin. Similar fire conditions and pollen composition was reported at Chalco as well as at the adjacent high-altitude Lerma basin during the MIS2 by Torres-Rodríguez et al. (2015) and Lozano-García et al. (1993, 2005). The second factor corresponds to low values of spring insolation along MIS6. Currently, spring insolation is associated with natural forest fires in the Basin of Mexico (CONAFOR, 2020).

A similar response in the low fire-activity signal and non-arboreal communities abundance was reported for MIS 6 in temperate records from North America such as Lake Baldwin (California, USA; Glover et al., 2017, 2020), Ziegles Reservoir (Colorado, USA; Anderson et al., 2020) and Lake Bear (Utah, USA; Kaufman et al., 2009), as well as in a record from Lake Biwa in Japan (Inoue et al., 2018) and the marine record MD45-2042 from southwestern Iberia (Daniau et al., 2007).

As previously reported by Ortega-Guerrero et al. (2020) in a multi-proxy approach including diatoms content, mineral magnetism and geochemistry, the aquatic ecosystem changed quickly during the end of MIS6 (ca. 132–130 ka). Our study confirms the indication of relatively short-term alternation between moister and drier climates with Ti, TIC, and C/N fluctuations and lower to higher forest cover and fire events.

5.2.2. Marine Isotope Stage 5 (130–72 ka; 106–57.5 m)

Previous work suggests that the lake level in Chalco dropped during MIS5 resulting in a shallow, rich-carbonate and oxic lake (Ortega-Guerrero et al., 2020). While the regional climate was generally dry and warm during this period, it was punctuated by times of less arid and cooler conditions (Ortega-Guerrero et al., 2020). Data here presented (Unit 6; Fig. 4) reveals considerable fluctuations during the substages of MIS5.

5.2.2.1. Sub-stage 5e (130-122 ka; 106–102 m). Sub-stage 5e appears to have had conditions similar to those between 145.2 and 143 ka. C/N

data suggests increasing proportions of terrestrial organic matter input into the lake. However, Ti data shows lower runoff. Therefore, enhanced input of terrestrial organic matter being washed into the basin seems a bit unlikely. Moreover, TIC data reflects relatively higher evaporation rates. Because of that, we suggest that increasing values of C/N might be reflecting the appearance of emergent plants on littorals with higher C/N signal (Cohen, 2003; Chávez-Lara et al., 2019) due to possible shallower conditions as TIC data suggests. This correlates well with previous diatom record dominated by alkaliphilous and halophilous in Chalco that documents increasing salinity and lowering lake level (Ortega-Guerrero et al., 2020). CHAR values increase to 24.1 mm^2/cm^2yr and the Z-Score reveals seven peaks that correlate with increasing TIC concentration at the beginning of this sub-stage. The high percentage of primary charcoal found in this section suggests that these are associated with local fires, and the high CHAR indicates an increase in fire-activity, possibly due to the increase in the spring insolation. Pollen data reveals an increase in forest cover at 130 ka, contributing to fuel availability and being consistent with the observed increase in charcoal. The surrounding terrestrial ecosystem changed considerably during MIS5e with an expansion of the forests between 127 and 125 ka and with evidence of local fires, in contrast with other tropical sites such as Lake Titicaca (Peru; Hanselman et al., 2005), Lake Fuquene (Colombia; Bogotá et al., 2011) and El Valle (Panama; Cárdenes-Sandí et al., 2019) where grassland communities and low fire-activity have been reported.

5.2.2.2. Sub-stage 5d (122–109 ka; 102–90 m). During sub-stage 5d, lower C/N values suggest increasing lake productivity as runoff input seems to enhance, based on relatively increasing Ti concentration. We suggest aquatic conditions favored lake productivity, especially around 120 ka, as more oxygenated runoff water got into the lake. However, after 119 ka, terrestrial organic matter input seems to increase (higher C/N values) correlating with increasing runoff based on Ti data. Furthermore, the lower TIC concentration in the record suggests fresher water likely associated with a low evaporation rate. According to the pollen data, forest cover diminished during this stage in comparison with the end of the previous period. CHAR values also increase during this period and Z-Score reveals 21 peaks associated with local fires. Although Z-Score analysis can distinguish local fires (Power et al., 2008), our data indicates a high percentage of secondary charcoal signal (>60%) in all the Z-Score peaks, as well as adverse environmental conditions for fire-activity such as low insolation values and relatively low forest cover suggested by high percentage of non-arboreal pollen. Although, we also consider the possibility of high charcoal particle delivery through runoff.

5.2.2.3. Sub-stage 5c (109–97 ka; 90–80.9 m). During sub-stage 5c, C/N values suggest that organic matter input was dominated by terrestrial components from 109 to 100 ka, whereas during the latter of this sub-stage, the sources shifted to a mixture of lacustrine and terrestrial vegetation. More variable Ti values might suggest a period of variable runoff input, but with drier conditions than during MIS5d. This is consistent with increased TIC concentration, suggesting higher evaporation rates. However, low CHAR values and two Z-Score peaks between 109 and 100 ka suggest reduction of local fires. The low fire-activity incidence at the beginning of the period from 109 to 100 ka might be the result of scarce fuel available, as pollen data suggest increased herbaceous communities. Towards the end of sub-stage 5c (100–97 ka), increasing fire-activity was recorded, along with higher TIC concentration than at the beginning of MIS5c, suggesting a higher evaporation rate and a significant burning of vegetation.

5.2.2.4. Sub-stage 5b (97–87 ka; 80.9–71.9 m). During sub-stage 5b, C/N values varied from 10 to 20, suggesting that organic matter in the lake was made up of relatively similar proportions of lacustrine and terrestrial vegetation. This was accompanied by increased Ti suggesting relatively higher runoff input than MIS5c. Lower TIC concentrations indicate lower evaporation rate conditions, which might have enhanced the aquatic productivity. However, a sudden increase in carbon flux and 27 detected Z-Score peaks indicate more local fires. Increasing fire-activity during this period seems to be linked to a gradual change of vegetation communities, such as the establishment of arboreal vegetation which probably worked as available fuel. Moreover, this was a time of increasing spring insolation, which would also enhance fire-activity. However, similar to the case of sub-stage 5d, we do not rule out the possibility that secondary charcoal could be associated with increased runoff.

5.2.2.5. Sub-stage 5a (87–72 ka; 71.9–57.5 m). Sub-stage 5a represents a period of higher variability in proxy records. C/N values suggest that terrestrial vegetation input dominated in the lake, especially during 80–77 ka and 73–71 ka, with higher runoff input, suggested by relatively high levels of Ti. Moreover, increasing TIC concentrations suggest increasing evaporation rate after 77 ka. Sediments representing this sub-stage reflect the highest CHAR of MIS5. Optimal conditions for fire recurrence occurred during this period. Forty-four Z-Score peaks in this period are associated with local fires and represent the shortest fire recurrence intervals of the entire record. According to the pollen data, the dominant vegetation is represented by forests (80–90%), a similar palynological data is recorded for the Holocene pollen records in Chalco (Lozano-García et al., 1993; Lozano and Ortega, 1998; Caballero et al., 2010) which suggest up-slope forest migration. Forest expansion likely provided sufficient fuel for fires during this sub-stage. Increases in spring insolation with low summer isolation could have promoted dryness during the summer and higher temperatures in the spring which can explain fire frequencies during this period.

5.2.3. Marine Isotope Stage 4 (72–56 ka; 57.5–41.1 m)

Previous studies of MIS4 in Chalco pointed out the alternation of Chalco limnological characteristics from a shallow, alkaline, saline lake with a high evaporation rate to a freshwater lake with a low evaporation rate (Ortega-Guerrero et al., 2020). Moreover, this period seems to have been dominated by cold conditions, although not as cold as during MIS6 (Ortega-Guerrero et al., 2020).

In the CHA08 record of MIS4 (57.5–41.1 m; Unit 5) C/N values suggest productive lake conditions with significant input of terrestrial vegetation. However, between 65 and 64 ka the terrestrial signal became dominant, corresponding to a drop in Ti with a corresponding enhancement in TIC concentration that together indicate less runoff and a higher evaporation rate. Therefore, we infer that at ca. 64 ka the lake level dropped, triggering the appearance of emergent plants with a terrestrial C/N signal (e.g. Chávez-Lara et al., 2019). After 63 ka, a rise in Ti and drop in TIC suggest that the lake level might have risen with increased runoff.

CHAR data show twenty-seven recognized Z-Score peaks that can be divided into two groups. The first group includes 10 peaks (72–64 ka; 57.5–52.5 m) associated with local fires and high fire-activity. This could have resulted from enhanced spring insolation, fuel availability based on high percentage of arboreal communities (>95%), and relatively dry conditions and high evaporation rate as previously discussed. The second group corresponds to 17 peaks (64–56 ka; 52.5–41.1 m) associated with local fires. However, CHAR is reduced (maximum point of 39.9 mm^2/cm^2yr), suggesting a diminished fire-activity in the Chalco area, possibly due to lower spring insolation.

5.2.4. Marine Isotope Stage 3 (56–35 ka; 41.1–29 m)

This section extends through most of MIS3, covering the period of 56 to 35 ka. During this period, Lake Chalco's limnological characteristics were similar to those of MIS4, with the lake varying between alka-

line-saline and freshwater conditions. Climate was dry and cold but warmer than during MIS4 (Ortega-Guerrero et al., 2020). High fire-activity has been reported in the area during this period (Torres-Rodríguez et al., 2015;).

C/N values suggest conditions of a productive lake, especially at 50 and 52 ka with a constant input of terrestrial organic matter, which is consistent with the low amplitude variations observed in Ti, possibly indicating relatively more stable runoff input. However, a high and variable evaporation rate is suggested by TIC concentration (0.1–4.3%). CHAR and Z-Score data reveal two significant peak groups. The first group is composed of 17 peaks associated with local fires from 57 to 47 ka (41.1–38 m) and with a low carbon flux (0–18.5 mm^2/cm^2yr). The relatively low fire-activity during the first part of MIS3 seems similar to the fire-activity recorded at MIS4. Forest cover is high, with no important changes. The spring insolation curve exhibits lower amplitude oscillation, but its mean values are higher than those present late in MIS4, representing a positive factor for fire-activity. On the other hand, the second group of charcoal peaks is composed of 33 peaks associated with local fires from 47 to 35 ka (38–29 m). During this period, the charcoal flux rose (0.1–63.5 mm^2/cm^2yr), but it was not as high as during sub-stage 5a. We thus suggest that environmental conditions were optimal for enhanced fire-activity with high arboreal pollen taxa (>90%), providing the necessary fuel.

5.3. North Hemisphere climatic forces in Lake Chalco

Several studies have proposed that glacial-interglacial cycles during the last 2.5 Myr are strongly linked to terrestrial changes. In particular, the 100 kyr eccentricity cycle has been clearly identified on marine and ice-core records (Raymo et al., 1989; Raymo, 1992; Schimidt and Spero, 2011). For example, climatic responses in southwestern North America and Central American during Termination II and the MIS5 transition, have been identified in several lacustrine records (e.g. Kaufman et al., 2009; Macario-Gonzalez 2017; Cárdenes-Sandí et al., 2019). Lake Chalco adds to this body of knowledge as it has recorded changes in the aquatic environment during MIS6-5 transition (Avendaño-Villeda et al., 2018; Ortega-Guerrero et al., 2020). Furthermore, data presented reveals gradual but significant variations on terrestrial ecosystems regarding fire-activity, vegetation composition, organic matter availability and runoff. Similar changes have also been reported in Lake Chalco during MIS2-1 transition (Torres-Rodríguez et al., 2015; Caballero et al., 2019). Spectral analysis carried out on Ti data reveals a statistical significant periodicity of 40–28 kyr (Fig. 5). However, we consider it dubious due to the relatively short temporality of our record (111 kyr). A cycle of 20 kyr (±2 kyr; Fig. 5) could be indicative of precessional forcing of runoff variation in Lake Chalco. A 23 kyr cyclicity for the ITZC mean latitudinal migration over the last 350 kyr has been reported in $\delta^{18}O$ marine records from the Caribbean (e.g. Schimidt and Spero, 2011), and this is a plausible mechanism as the driver of the observed variations in Chalco runoff. Several studies have suggested that these ITCZ migrations are mainly produced by variation of the energetic balance determined by summer insolation (Schneider et al., 2014), particularly at 65°N (Bosmans et al., 2015; Lachniet et al., 2014). However, during short time scale periods (e.g. Holocene) other factors may also influence the ITCZ mean position (6°N currently) such as the Pacific and Atlantic SST, solar irradiance and teleconnections (e.g. Pacific Decadal Oscillation, El Niño South Oscillation) (Magaña et al., 2003; Knight et al., 2006; Metcalfe et al., 2015).

Lake Chalco runoff results (based on Ti concentration) are congruent with other sedimentary records such as Lake Baldwin (Glover et al., 2017), Cariaco Basin (Yarincik et al., 2000), and the equatorial record of 1239 ODP site (Rincón-Martínez et al., 2010), along a North-South transect from North and Central America (Fig. 6). These results might be evaluated in the context of changes in 65°N summer insolation, which has a significant impact on ITZC position, as discussed above

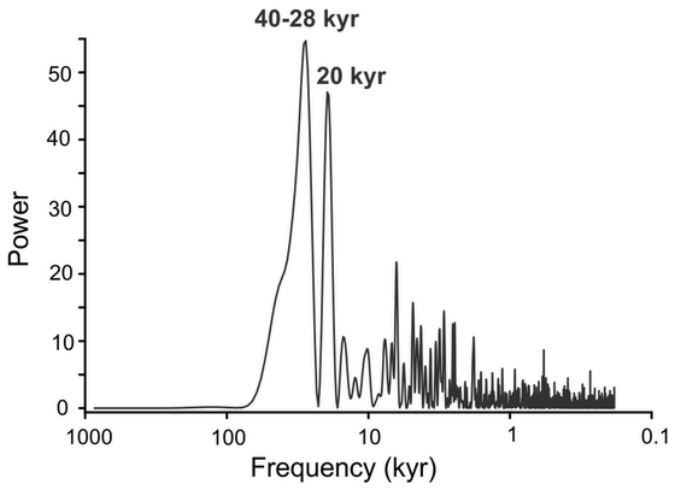

Fig. 5. Spectral analysis of Ti data from 143 to 35 ka using the Lomb periodogram algorithm for unevenly sampled data from Past software (Hammer et al., 2001). The analysis shows three main periodicities. The cycle of 20 ± 2 kyr is associated with the precessional cycle. Frequency highest peaks are indicated.

(Bosmans et al., 2015; Lachniet et al., 2014). Previous works have suggested wet conditions in temperate regions during MIS6 (e.g. Kaufman et al., 2009), whereas dry environments have been reported in tropical regions for this period (e.g. Bogotá et al., 2011; Cárdenes-Sandí et al., 2019). The MIS 6 record in the Chalco shows general wet conditions punctuated by drier episodes (e.g. 143 ka), as well as a tendency to a sudden increase of runoff (e.g. 132 ka) with a clear dry episode at the end of the period (e.g. 130 ka). The precipitation distribution model of Metcalfe et al. (2015) compares various sites from North and Central America showing that the end of MIS2 (12.9–11.6 ka) was characterized by opposite conditions to those we propose for the end of MIS6. This model suggests that ca. 12 ka the ITCZ was in a southern location, depriving moisture to southern Mexico and Central America during this period. In contrast, records from northern Mexico and the southern United States indicate that these mid-latitude areas were impacted by precipitation associated with strong Pacific westerly activity during the same time. We suggest that an opposite set of conditions may have occurred during 134–130 ka, leading to increased runoff at Lake Chalco during the MIS6-5e.

Coastal marine records (1239 ODP and Cariaco Basin) appear to be more responsive to ITCZ shifts (Fig. 6), recording sudden terrestrial input changes during MIS5, particularly in the MIS5e and MIS5c periods (Yarincik et al., 2000; Rincón-Martínez et al., 2010). In comparison, the Chalco record also shows a trend of increasing runoff with subtle variation during MIS5e. We note that this response in runoff appears to have a delay relative to the equatorial records, consistent with the hypothesized ITCZ migration mechanism, but recognize that our chronological control is insufficient for definite conclusions of the relative timing of events in these records. Finally, during MIS5a, MIS4 and MIS3, the datasets do not show clear correlation. We suggest that other regional atmospheric-oceanic factors (e.g. Pacific and Atlantic SST) may be affecting the runoff conditions in these sites as Metcalfe et al. (2015) have suggested for the Mid Holocene.

6. Conclusions

In this paper, we explored the responses of Lake Chalco productivity, forest cover and fire history at the high tropical altitude of the Basin of Mexico from 146 to 35 ka. We used total organic Carbon to total Nitrogen ratio (C/N) as a marker of organic matter source, the total inorganic Carbon concentration as an indicator of evaporation rate, and Titanium content as an indicator of runoff. Forest cover was recon-

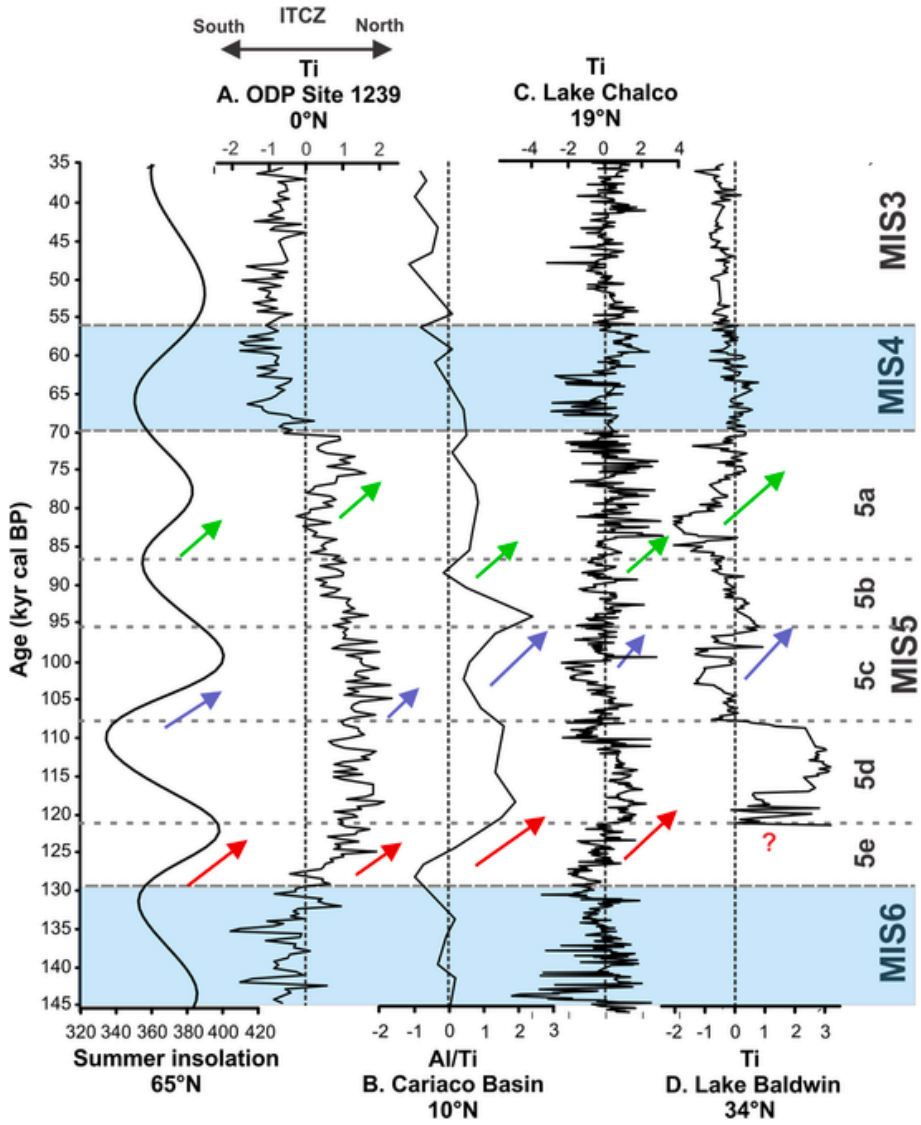

Fig. 6. Comparison of summer insolation at 65°N with terrigenous input proxies from regional records. A) Ecuador (1239 ODP site; Rincón-Martínez et al., 2010), B) Cariaco Basin (Yarincik et al., 2000), C) Lake Chalco (this study) and D) Lake Baldwin in California-USA (Glover et al., 2017). Proxies are shown as standardized data. Marine Isotopic Stages and sub-stages are marked. Colored arrows indicate the record response to increasing summer insolation: red) MIS6-5e transition, blue) MIS5d-c stages, and green) MIS5a sub-stage. The lengths of colored arrows correspond to the duration of periods of increasing isolation or terrigenous inputs. (For interpretation of the references to color in this figure legend, the reader is referred to the Web version of this article.)

structed based on arboreal and non-arboreal pollen data. Charcoal accumulation rate (CHAR) and the Z-Score analysis were estimated to determine fire-activity, the latter used for the first time in Central Mexico.

Our main findings are the conditions between 146 and 130 ka (end of MIS6) corresponding to a highly productive lake with low evaporation rate. At the basin, poor forest-cover with low fire recurrence is recorded. A short period of shallow lake level with a decrease in runoff and lake productivity, and increased charcoal accumulation suggest a rapid change during the MIS5e transition. Dry conditions occurred during the MIS5e, with low runoff and a period with high forest cover between 127 and 125 ka. The charcoal records indicate the occurrence of local fires.

For the MIS 5, pollen data and charcoal accumulation rate indicate a trend towards an increase in the forest cover with periods of fire-activity during the MIS 5d, 5b, and 5a, the latter related to higher spring insolation. Even the peak signal detected by Z-Score analysis, the MIS 5d fire record could correspond to carry-over of carbonized particles by runoff and not to fire activity. The lake productivity was variable and dry conditions were reconstructed for the MIS5c. The Chalco record shows that during MIS 4, the interval between 72 and 65 ka was dry with few fire events; this period corresponds to high spring insolation. After 63 ka an increase on runoff was recorded. The MIS 3 reveals low amplitude variations in runoff, lake productivity, evaporation rate and fire activity, despite high forest cover from 56 to 47 ka. After 47 ka, episodes of high evaporation rate and high fire-activity with evidence of local fires are documented.

The spectral analysis performed on Ti concentration data reveals a 20 ± 2 ka cyclicity. We suggest this might correspond to the precessional forcing reflected on runoff variation in Chalco. We hypothesize that the ITCZ migration with a 23 ka cyclicity might be the probable mechanism for explaining runoff changes in Chalco. A visual comparison from Lake Chalco runoff results with other sedimentary records from North and Central America, and the 65°N summer insolation previously proposed impacting the ITCZ, reflect a similar pattern for the MIS 6 to MIS 5 transition.

Uncited references

Comisió n Nacional Forestal [CONAFOR], 2020, Shackleton, 1967.

Declaration of competing interest

The authors declare that they have no known competing financial interests or personal relationships that could have appeared to influence the work reported in this paper.

Acknowledgements

This research was funded by UNAM DGAPA-PAPIIT IN103819 and by the US NSF (EAR-1462347). XRF core scanning was performed at the Large Lakes Observatory, University of Minnesota-Duluth. We would like to thank the authorities of the Ejido Tulyehualco for the support and access to the drilling site. Also we thank the technicians and students who helped during the different analysis: Martín Hernández, Karla Zurizadae, Minerva López and Erandí Rodríguez.

References

Anderson, R.S., Jiménez-Moreno, G., Belanger, M., Briles, C., 2020. Fire history of the unique high-elevation Snowmastodon (Ziegler Reservoir) site during MIS 6–4, with comparisons of TII to TI in the southern Colorado Rockies. Quat. Sci. Rev. 232, 106–213. https://doi.org/10.1016/j.quascirev.2020.106213.

Arce, J.L., Layer, P.W., Macías, J.L., Morales-Casique, E., García-Palomo, A., Jiménez-Domínguez, F.J., et al., 2019. Geology and stratigraphy of the Mexico basin (Mexico City), central Trans-Mexican volcanic Belt. J. Maps 15 (2), 320–332. https://doi.org/10.1080/17445647.2019.1593251.

Arce, J.L., Macías, J.L., Vázquez-Selem, L., 2003. The 10.5 ka Plinian eruption of Nevado de Toluca volcano, Mexico: stratigraphy and hazard implications. Geol. Soc. Am. Bull. 115 (2), 230–248. https://doi.org/10.1130/0016-7606(2003)115%3C0230:TKPEON%3E2.0.CO;2.

Avendaño-Villeda, D.A., Caballero, M., Ortega-Guerrero, B., Lozano-García, S., Brown, E., 2018. Condiciones ambientales a finales del Estadio Isotópico 6 (EI 6: > 130000 años) en el centro de Mexico: caracterización de una sección de sedimentos laminados proveniente del Lago de Chalco. Rev. Mex. Ciencias Geol. 35 (2), 168–178. https://doi.org/10.22201/cgeo.20072902e.2018.2.649.

Batten, D.J., 1999. Small palynomorphs. In: Jones, T.P., Rowe, N.P. (Eds.), Fossil Plants and Spores: Modern Techniques. The Geological Society, London, pp. 15–19.

Blaauw, M., Christen, J.A., 2011. Flexible paleoclimate age-depth models using an autoregressive gamma process. Bayesian analysis 6 (3), 457–474. https://doi.org/10.1214/11-BA618. https://projecteuclid.org/euclid.ba/1339616472.

Bogotá, R.G., Groot, H.M., Hooghiemstra, H., Lourens, L.J., Van der Linden, M., Berrio, J.C., 2011. Rapid climate change from north Andean Lake Fuquene pollen records driven by obliquity: implications for a basin-wide biostratigraphic zonation for the last 284 ka. Quat. Sci. Rev. 30 (23–24), 3321–3337. https://doi.org/10.1016/j.quascirev.2011.08.003.

Bosmans, H.C., Hilgen, F.J., Tuenter, E., Lourens, L.J., 2015. Obliquity forcing of low-latitude climate. Clim. Past 11 (10), 1335–1346. https://doi.org/10.5194/cp-11-1335-2015.

Boyle, J.F., 2002. Inorganic geochemical methods in palaeolimnology. In: Last, W.M., Smol, J.P. (Eds.), Tracking Environmental Change Using Lake Sediments, vol. 2. Springer, Dordrecht, pp. 83–141.

Brown, E.T., Caballero, M., Cabral Cano, E., Fawcett, P.J., Lozano-García, S., Ortega, B., et al., 2019. Scientific drilling of lake Chalco, Basin of Mexico (MexiDrill). Sci. Drill. 26. https://doi.org/10.5194/sd-26-1-2019.

Brücher, T., Brovkin, V., Kloster, S., Marlon, J.R., Power, M.J., 2014. Comparing modelled fire dynamics with charcoal records for the Holocene. Clim. Past 10 (2), 811–824. https://doi.org/10.5194/cp-10-811-2014.

Bush, M.B., Correa-Metrio, A.Y., Hodell, D.A., Brenner, M., Anselmetti, F.S., Ariztegui, D., et al., 2009. Re-evaluation of climate change in lowland Central America during the Last Glacial Maximum using new sediment cores from Lake Petén Itzá, Guatemala. In: Vimeux, F., Sylvestre, F., Khodri, M. (Eds.), Past Climate Variability in South America and Surrounding Regions: from the Last Glacial Maximum to the Holocene, vol. 14. Springer, Dordrecht, pp. 113–128. https://doi.org/10.1007/978-90-481-2672-9_5.

Caballero, M., Lozano-García, S., Ortega-Guerrero, B., Correa-Metrio, A., 2019. Quantitative estimates of orbital and millennial scale climatic variability in central Mexico during the last ~ 40,000 years. Quat. Sci. Rev. 205, 62–75. https://doi.org/10.1016/j.quascirev.2018.12.002.

Caballero, M., Lozano-García, S., Vázquez-Selem, L., Ortega, B., 2010. Evidencias de cambio climático y ambiental en registros glaciales y en cuencas lacustres del centro de Mexico durante el último máximo glacial. Bol. Soc. Geol. Mex. 62 (3), 359–377. http://www.scielo.org.mx/scielo.php?script=sci_arttext&pid=S1405-33222010000300005&lng=es&nrm=iso.

Cai, Y., Cheng, H., An, Z., Edwards, R.L., Wang, X., Tan, L., Wang, J., 2010. Large variations of oxygen isotopes in precipitation over south-central Tibet during Marine Isotope Stage 5. Geology 38 (3), 243–246. https://doi.org/10.1130/G30306.1.

Cárdenes-Sandí, G.M., Shadik, C.R., Correa-Metrio, A., Gosling, W.D., Cheddadi, R., et al., 2019. Central American climate and microrefugia: a view from the last interglacial. Quat. Sci. Rev. 205, 224–233. https://doi.org/10.1016/j.quascirev.2018.12.021.

Chávez-Lara, C.M., Holtvoeth, J., Roy, P.D., Pancost, R.D., 2019. Lipid biomarkers in lacustrine sediments of subtropical northeastern Mexico and inferred ecosystem changes during the late Pleistocene and Holocene. Palaeogeography, Palaeoclimatology. Palaeoecology 535, 109–343. https://doi.org/10.1016/j.palaeo.2019.109343.

Clark, J.S., Royall, P.D., 1996. Local and regional sediment charcoal evidence for fire regimes in presettlement north-eastern North America. J. Ecol. 365–382. https://doi.org/10.2307/2261199.

Cohen, A.S., 2003. Paleolimnology: the History and Evolution of Lake Systems. Oxford University Press. https://doi.org/10.1669/0883-1351(2004)019%3C0184:BR%3E2.0.CO;2.

Comisión Nacional Forestal [CONAFOR] Reporte semanal nacional de Incendios forestales al 7/05/2020 https://www.gob.mx/conafor/documentos/reporte-semanal-de-incendios 2020

Daniau, A.L., Sánchez-Goñi, M.F., Beaufort, L., Laggoun-Défarge, F., Loutre, M.F., Duprat, J., 2007. Dansgaard–Oeschger climatic variability revealed by fire emissions in southwestern Iberia. Quat. Sci. Rev. 26 (9–10), 1369–1383. https://doi.org/10.1016/j.quascirev.2007.02.005.

Dansgaard, W., Johnsen, S.J., Clausen, H.B., Dahl-Jensen, D., Gundestrup, N.S., Hammer, C.U., et al., 1993. Evidence for general instability of past climate from a 250-kyr ice-core record. Nature 364 (6434), 218–220.

Emiliani, C., 1955. Pleistocene temperatures. J. Geol. 63 (6), 538–578. https://doi.org/10.1086/626295.

García-Palomo, A., Macías, J.L., Arce, J.L., Capra, L., Garduño, V.H., Espíndola, J.M., 2002. Geology of Nevado de Toluca Volcano and surrounding areas, central Mexico. Colorado. Geological Society of America Map and Chart Series MCH089, 26, Boulder.

Glantz, S.A., Slinker, B.K., Neilands, T.B., 2016. Primer of Applied Regression & Analysis of Variance. third ed. McGraw Hill.

Glover, K.C., Chaney, A., Kirby, M.E., Patterson, W.P., MacDonald, G.M., 2020. Southern California vegetation, wildfire, and erosion had nonlinear responses to climatic forcing during marine isotope stages 5–2 (120–15 ka). Paleoceanography and Paleoclimatology 35 (2), 28–36. https://doi.org/10.1029/2019PA003628.

Glover, K.C., MacDonald, G.M., Kirby, M.E., Rhodes, E.J., Stevens, L., Silveira, E., et al., 2017. Evidence for orbital and North Atlantic climate forcing in alpine Southern California between 125 and 10 ka from multi-proxy analyses of Baldwin Lake. Quat. Sci. Rev. 167, 47–62. https://doi.org/10.1016/j.quascirev.2017.04.028.

Google Earth Pro, 2020. P. Icture Date: 01/15/2015. Maxat Technologies Images.

Guiter, F., Andrieu-Ponel, V., Beaulieu, J.L., Cheddadi, R., Calvez, M., Ponel, P., et al., 2003. The last climatic cycles in Western Europe: a comparison between long continuous lacustrine sequences from France and other terrestrial records. Quat. Int. 111 (1), 59–74. https://doi.org/10.1016/S1040-6182(03)00015-6.

Hammer, Ø., Harper, D.A., Ryan, P.D., 2001. PAST: paleontological statistics software package for education and data analysis. Palaeontol. Electron. 4 (1), 9. http://folk.uio.no/ohammer/past/.

Hanselman, J.A., Bush, M.B., Gosling, W.D., Collins, A., Knox, C., Baker, P.A., Fritz, S.C., 2011. A 370,000-year record of vegetation and fire history around Lake Titicaca (Bolivia/Peru). Palaeogeography, Palaeoclimatology,. Palaeoecology 305 (1–4), 201–214. https://doi.org/10.1016/j.palaeo.2011.03.002.

Hanselman, J.A., Gosling, W.D., Paduano, G.M., Bush, M.B., 2005. Contrasting pollen histories of MIS 5e and the Holocene from Lake Titicaca (Bolivia/Peru). J. Quat. Sci.: Published for the Quaternary Research Association 20 (7–8), 663–670. https://doi.org/10.1002/jqs.979.

Heusser, L., Oppo, D., 2003. Millennial-and orbital-scale climate variability in southeastern United States and in the subtropical Atlantic during Marine Isotope Stage 5: evidence from pollen and isotopes in ODP Site 1059. Earth Planet Sci. Lett. 214 (3–4), 483–490. https://doi.org/10.1016/S0012-821X(03)00389-3.

Higuera, P.E., Peters, M.E., Brubaker, L.B., Gavin, D.G., 2007. Understanding the origin and analysis of sediment-charcoal records with a simulation model. Quat. Sci. Rev. 26 (13–14), 1790–1809. https://doi.org/10.1016/j.quascirev.2007.03.010.

Instituto Nacional de Estadística, Geografía e Informática [INEGI], 2020. Continuo Mexicano de Elevaciones. https://www.inegi.org.mx/app/geo2/elevacionesmex/.

Inoue, J., Okuyama, C., Takemura, K., 2018. Long-term fire activity under the East Asian monsoon responding to spring insolation, vegetation type, global climate, and human impact inferred from charcoal records in Lake Biwa sediments in central Japan. Quat. Sci. Rev. 179, 59–68. https://doi.org/10.1016/j.quascirev.2017.11.007.

Kaufman, D.S., Bright, J., Dean, W.E., Rosenbaum, J.G., Moser, K., Anderson, R.S., et al., 2009. A quarter-million years of paleoenvironmental change at bear lake, Utah and Idaho. Paleoenvironments of bear lake, Utah and Idaho, and its catchment,(rosembaum, JG, kaufman, DS, eds.). Geological Society of America Special 450, 311–351. https://doi.org/10.1130/2009.2450(14).

Kirby, M.E., Lund, S.P., Patterson, W.P., Anderson, M.A., Bird, B.W., Ivanovici,

L., et al., 2010. A Holocene record of Pacific decadal oscillation (PDO)-related hydrologic variability in southern California (Lake Elsinore, CA). J. Paleolimnol. 44 (3), 819–839. https://doi.org/10.1007/s10933-010-9454-0.
Knight, J.R., Folland, C.K., Scaife, A.A., 2006. Climate impacts of the Atlantic multidecadal oscillation. Geophys. Res. Lett. 33, L17706. https://doi.org/10.1029/2006GL026242.
Lachniet, M.S., Denniston, R.F., Asmerom, Y., Polyak, V.J., 2014. Orbital control of western North America atmospheric circulation and climate over two glacial cycles. Nat. Commun. 5 (1), 1–8. https://doi.org/10.1038/ncomms4805.
Leunda, M., Gil-Romera, G., Daniau, A.L., Benito, B.M., González-Sampériz, P., 2020. Holocene fire and vegetation dynamics in the Central Pyrenees (Spain). Catena 188, 104–411. https://doi.org/10.1016/j.catena.2019.104411.
Lisiecki, L.E., Raymo, M.E., 2005. A Pliocene-Pleistocene stack of 57 globally distributed benthic δ18O records. Paleoceanography 20 (1). https://doi.org/10.1029/2004PA001071.
Long, C.J., Whitlock, C., Bartlein, P.J., Millspaugh, S.H., 1998. A 9000-year fire history from the Oregon Coast Range, based on a high-resolution charcoal study. Can. J. For. Res. 28 (5), 774–787.
Lopez-Perez, M., 2014. Material carbonizado en registros lacustres como indicador de regímenes de incendios en el centro y sur del país. Bachelor thesis. National Autonomous University of Mexico.
Lozano-Garcia, M.S., Ortega-Guerrero, B., Caballero-Miranda, M., Urrutia-Fucugauchi, J., 1993. Late pleistocene and Holocene paleoenvironments of Chalco lake, central Mexico. Quat. Res. 40 (3), 332–342. https://doi.org/10.1006/qres.1993.1086.
Lozano-García, M.S., 1996. La vegetación Cuaternaria en el Centro de Mexico: registros Palinológicos e Implicaciones Paleoclimáticas. Bol. Soc. Bot. Mex. 58, 113–127. https://doi.org/10.17129/botsci.1492.
Lozano, S., Ortega, B., 1998. Late Quaternary environmental changes of the central part of the Basin of Mexico; correlation between Texcoco and Chalco basins. Rev. Palaeobot. Palynol. 99 (2), 77–93. https://doi.org/10.1016/S0034-6667(97)00046-8.
Lozano-García, S., Sosa-Nájera, S., Sugiura, Y., Caballero, M., 2005. 23,000 yr of vegetation history of the Upper Lerma, a tropical high-altitude basin in Central Mexico. Quat. Res. 64 (1), 70–82. https://doi.org/10.1016/j.yqres.2005.02.010.
Lozano-García, S., Ortega, B., Roy, P.D., Beramendi-Orosco, L., Caballero, M., 2015. Climatic variability in the northern sector of the American tropics since the latest MIS 3. Quat. Res. 84 (2), 262–271. https://doi.org/10.1016/j.yqres.2015.07.002.
Lozano-García, S., Brown, E.T., Ortega, B., Caballero, M., Werne, J., Fawcett, P.J., et al., 2017. Perforación profunda en el lago de Chalco: reporte técnico. Bol. Soc. Geol. Mex. 69 (2), 299–311. https://doi.org/10.18268/bsgm2017v69n2a2.
Macario-Gonzalez, L., 2017. Environmental history of the last 400,000 years in the northern neotropical region based on lake petén itzá sediments Ph.D. Thesis technischen universität carolo-wilhelmina.
Magaña, V.O., Vázquez, J.L., Pérez, J.L., Pérez, J.B., 2003. Impact of el Niño on precipitation in Mexico. Instituto de Geofísica 42, 313–330. https://www.redalyc.org/articulo.oa?id=56842304.
Martínez-Abarca, L.R., 2019a. Lago de Chalco: registro sedimentario y estratigráfico de sus etapas formativas). Master thesis. National Autonomous University of Mexico.
Martínez-Abarca, R., Lozano-García, S., Ortega-Guerrero, B., Caballero-Miranda, M., 2019b. Incendios y actividad volcánica: historia de fuego en la cuenca de Mexico en el Pleistoceno tardío con base en registros de material carbonizado en el lago de Chalco. Rev. Mex. Ciencias Geol. 36 (2), 259–269. https://doi.org/10.22201/cgeo.20072902e.2019.2.1090.
Mason, C.B., Moore, 1982. Principles of Geochemistry. Wiley, New York, Singapore.
Metcalfe, S.E., Barron, J.A., Davies, S.J., 2015. The Holocene history of the North American Monsoon: 'known knowns' and 'known unknowns' in understanding its spatial and temporal complexity. Quat. Sci. Rev. 120, 1–27. https://doi.org/10.1016/j.quascirev.2015.04.004.
Meyers, P.A., Ishiwatari, R., 1995. Organic Matter Accumulation Records in Lake Sediments. In: Lerman, A., Imboden, D.M., Gat, J.R. (Eds.), Physics and Chemistry of Lakes. Springer, Berlin, pp. 279–328. https://doi.org/10.1007/978-3-642-85132-2_10.
Moreno, A., González-Sampériz, P., Morellón, M., Valero-Garcés, B.L., Fletcher, W.J., 2012. Northern Iberian abrupt climate change dynamics during the last glacial cycle: a view from lacustrine sediments. Quat. Sci. Rev. 36, 139–153. https://doi.org/10.1016/j.quascirev.2010.06.031.
Muhs, D.R., Wehmiller, J.F., Simmons, K.R., York, L.L., 2003. Quaternary sea-level history of the United States. Dev. Quat. Sci. 1, 147–183. https://doi.org/10.1016/S1571-0866(03)01008-X.
Oris, F., Ali, A.A., Asselin, H., Paradis, L., Bergeron, Y., Finsinger, W., 2014. Charcoal dispersion and deposition in boreal lakes from 3 years of monitoring: differences between local and regional fires. Geophys. Res. Lett. 41 (19), 6743–6752. https://doi.org/10.1002/2014GL060984.
Ortega-Guerrero, B., Avendaño, D., Caballero, M., Lozano-García, S., Brown, E.T., Rodríguez, A., et al., 2020. Climatic control on magnetic mineralogy during the late MIS 6-Early MIS 3 in Lake Chalco, central Mexico. Quat. Sci. Rev. 230, 106–163. https://doi.org/10.1016/j.quascirev.2020.106163.
Ortega-Guerrero, B., Lozano-García, S., Herrera-Hernández, D., Caballero, M., Beramendi-Orosco, L., Bernal, J.P., Torres-Rodríguez, E., Avendaño-Villeda, D., 2017. Lithostratigraphy and physical properties of lacustrine sediments of the last ca. 150 kyr from Chalco basin, central Mexico. J. S. Am. Earth Sci. 79, 507–524. https://doi.org/10.1016/j.jsames.2017.09.003.
Power, M.J., Marlon, J., Ortiz, N., Bartlein, P.J., Harrison, S.P., Mayle, F.E., et al., 2008. Changes in fire regimes since the Last Glacial Maximum: an assessment based on a global synthesis and analysis of charcoal data. Clim. Dynam. 30 (7–8), 887–907. https://doi.org/10.1007/s00382-007-0334-x.
Press, W.H., Teukolsky, S.A., Vetterling, W.T., Flannery, B.P., 1992. Numerical Recipes in. C. Cambridge University Press.
R Core Team, 2018. R: a language and environment for statistical computing. R Foundation for Statistical Computing. Austria, Vienna. https://www.R-project.org/.
Raymo, M.E., 1992. Global climate change: a three million year perspective. In: Kulda (Ed.), et al., Start of a Glacial. Springer, Berlin. pp. 207–223. https://doi.org/10.1007/978-3-642-76954-2_15.
Raymo, M.E., Ruddiman, W.F., Backman, J., Clement, B.M., Martinson, D.G., 1989. Late Pliocene variation in Northern Hemisphere ice sheets and North Atlantic deep water circulation. Paleoceanography 4 (4), 413–446.
Reimer, P.J., Bard, E., Bayliss, A., Beck, J.W., Blackwell, P.G., Ramsey, C.B., et al., 2013. IntCal13 and Marine13 radiocarbon age calibration curves 0–50,000 years cal BP. Radiocarbon 55 (4), 1869–1887. https://doi.org/10.2458/azu_js_rc.55.16947.
Rincón-Martínez, D., Lamy, F., Contreras, S., Leduc, G., Bard, E., Saukel, C., et al., 2010. More humid interglacials in Ecuador during the past 500 kyr linked to latitudinal shifts of the equatorial front and the Intertropical Convergence Zone in the eastern tropical Pacific. Paleoceanography 25 (2). https://doi.org/10.1029/2009PA001868.
Roy, P.D., Quiroz-Jiménez, J.D., Pérez-Cruz, L.L., Lozano-García, S., Metcalfe, S.E., Lozano-Santacruz, R., et al., 2013. Late Quaternary paleohydrological conditions in the drylands of northern Mexico: a summer precipitation proxy record of the last 80 cal ka BP. Quat. Sci. Rev. 78, 342–354. https://doi.org/10.1016/j.quascirev.2012.11.020.
Schmidt, M.W., Spero, H.J., 2011. Meridional shifts in the marine ITCZ and the tropical hydrologic cycle over the last three glacial cycles. Paleoceanography 26 (1). https://doi.org/10.1029/2010PA001976.
Schneider, T., Bischoff, T., Haug, G.H., 2014. Migrations and dynamics of the intertropical convergence zone. Nature 513 (7516), 45–53. https://doi.org/10.1038/nature13636.
Shackleton, N., 1967. Oxygen isotope analyses and Pleistocene temperatures re-assessed. Nature 215, 15–17.
Sosa-Ceballos, G., Gardner, J.E., Siebe, C., Macías, J.L., 2012. A caldera-forming eruption ~14,100 14C yr BP at Popocatépetl volcano, Mexico: insights from eruption dynamics and magma mixing. J. Volcanol. Geoth. Res. 213, 27–40. https://doi.org/10.1016/j.jvolgeores.2011.11.001.
Talbot, M.R., Johannessen, T., 1992. A high resolution palaeoclimatic record for the last 27,500 years in tropical West Africa from the carbon and nitrogen isotopic composition of lacustrine organic matter. Earth Planet Sci. Lett. 110 (1–4), 23–37. https://doi.org/10.1016/0012-821X(92)90036-U.
Tinner, W., Hu, F.S., 2003. Size parameters, size-class distribution and area-number relationship of microscopic charcoal: relevance for fire reconstruction. Holocene 13 (4), 499–505 https://doi.org/10.1191%2F0959683603hl615rp.
Torres-Rodríguez, E., Lozano-García, S., Caballero-Miranda, M., Ortega-Guerrero, B., Sosa-Nájera, S., et al., 2018. Pollen and non-pollen palynomorphs of Lake Chalco as indicators of paleolimnological changes in high-elevation tropical central Mexico since MIS 5. J. Quat. Sci. 33 (8), 945–957. https://doi.org/10.1002/jqs.3072.
Torres-Rodríguez, E., Lozano-García, S., Roy, P., Ortega, B., Beramendi-Orosco, L., Correa-Metrio, A., Caballero, M., 2015. Last Glacial droughts and fire regimes in the central Mexican highlands. J. Quat. Sci. 30 (1), 88–99. https://doi.org/10.1002/jqs.2761.
Vriend, M., Groot, M.H.M., Hooghiemstra, H., Bogotá-Angel, R.G., Berrio, J.C., 2012. Changing depositional environments in the Colombian Fuquene Basin at submillennial time-scales during 284-27 ka from unmixed grain-size distributions and aquatic pollen. Neth. J. Geosci. 91 (1–2), 199–214. https://doi.org/10.1017/S0016774600001591.
Watts, W.A., Allen, J.R.M., Huntley, B., 2000. Palaeoecology of three interstadial events during oxygen-isotope Stages 3 and 4: a lacustrine record from Lago Grande di Monticchio, southern Italy. Palaeogeography, Palaeoclimatology. Palaeoecology 155 (1–2), 83–93. https://doi.org/10.1016/S0031-0182(99)00096-6.
Whitlock, C., Millspaugh, S.H., 1996. Testing the assumptions of fire-history studies: an examination of modern charcoal accumulation in Yellowstone National Park, USA. Holocene 6 (1), 7–15 https://doi.org/10.1177%2F095968369600600102.
Whitlock, C., Larsen, C., 2001. Charcoal as a fire proxy. In: Last, W.M., Smol, J.P. (Eds.), Tracking Environmental Change Using Lake Sediments, vol. 3. Springer, Dordrecht, pp. 75–97.
Yang, X., Preusser, F., Radtke, U., 2006. Late Quaternary environmental changes in the Taklamakan Desert, western China, inferred from OSL-dated lacustrine and aeolian deposits. Quat. Sci. Rev. 25 (9–10), 923–932. https://doi.org/10.1016/j.quascirev.2005.06.008.
Yarincik, K.M., Murray, R.W., Peterson, L.C., 2000. Climatically sensitive eolian and hemipelagic deposition in the Cariaco Basin, Venezuela, over the past 578, 000 years: results from Al/Ti and K/Al. Paleoceanography 15 (2), 210–228. https://doi.org/10.1029/1999PA900048.